Bearing Starting Torque Measurements Down to -100°C

Kim Aaron*, Duval Johnson*, Shana Worel* and Frank Tao*

Abstract

Starting torque was measured for three different bearings from 0°C down to -90°C and -100°C. These were bearings of the type that will be used in the ice-penetrating radar instrument named Radar for Europa Assessment and Sounding: Ocean to Near-surface (REASON), which is part of the planned science instrument suite for the National Aeronautics and Space Administration (NASA) Europa Clipper mission. This space science mission to Jupiter's moon, Europa, is being led by NASA's Jet Propulsion Laboratory (JPL), which is administered for NASA by the California Institute of Technology. In addition to presenting the starting torque measurements at various temperatures, this paper describes the small test chamber and attachments that allowed the measurements to be made using an existing bearing torque testing machine.

Introduction

Bearings are used in the mechanisms that will deploy the REASON antennas. These antennas use stored strain energy in springs to provide the motive force that deploys the antennas. These antennas are designed, fabricated and tested mechanically by Heliospace Corp. in Berkeley, California under a subcontract to NASA/JPL.

During deployment of the antennas, the temperature may be as low as -70°C. There is a limited amount of data available regarding potential lubricants for operation at such low temperatures. Extrapolation of this data indicated that they could potentially provide the desired lubricating action, but the uncertainty was high so testing was performed to confirm the behavior of the lubricants at these temperatures.

At low temperatures, the viscosity of lubricants can increase by orders of magnitude. Because oil does not crystallize, or solidify, at any temperature, it technically does not freeze. However, at low enough temperatures it will lose its liquid-like properties and not flow enough to provide adequate lubrication. It was possible that the spring force available in the actuators would not be sufficient to overcome the low-temperature bearing resistance. We were confident that if the bearing was able to start turning, the shearing action in the lubricant would warm it locally, decreasing its viscosity, allowing the rolling action of the bearings to continue reliably. Therefore, we focused on measuring just the starting torque at various cold temperatures. These experimental measurements confirmed that the available mechanism torque was well above the measured starting torque even at temperatures that were colder than our expected worst-case cold deployment conditions. In addition, the testing confirmed that the volume of lubricant selected was appropriate for the short-duration one-time operation of the devices containing the tested bearing types.

In the body of this paper, we describe the three bearings tested, indicate the lubricant selected, illustrate the test apparatus, and present the results of starting torque versus temperature.

* California Institute of Technology, Jet Propulsion Laboratory, Pasadena, CA; Kim.M.Aaron@jpl.nasa.gov

Bearings Tested

We tested three bearings of the type selected for use in the design of the mechanism. Our colleague, Mark Balzer, named them Papa Bearing, Mama Bearing, and Baby Bearing because of their relative sizes. We fondly retained this nomenclature.

The three bearings tested are:

1. AST 07150776 (SSRI-1212ZZRA5P25L01 BEARING; MINO: 00585 X 74748)
   Approximate bearing dimensions: 19.05 mm outer diameter (OD) x 12.70 mm inner diameter (ID) x 3.94 mm width (W) (0.750 inch x 0.500 inch x 0.155 inch) (Papa bearing)
2. AST 07366778 (SSR3ZZRA5P25L01 INCH SERIES BEARINGS; MINO: 00585 X 00208)
   Approximate bearing dimensions: 12.70 mm OD x 4.70 mm ID x 4.95 mm W (0.500 inch x 0.185 inch x 0.195 inch) (Mama bearing)
3. AST 07366756 (SSR2ZZRA5P25L01 INCH SERIES BEARINGS; MINO: 00585 X 00187)
   Approximate bearing dimensions: 9.53 mm OD x 3.05 mm ID x 3.96-mm W (0.375 inch x 0.120 inch x 0.156 inch) (Baby bearing)

Manufacturer – New Hampshire Ball Bearing, Inc
Ring material – AISI 440C
Ball material – AISI 440C
Type – Radial
Shields – Double metallic shield, removable
Cage – Ribbon, land piloted
ABEC tolerance – ABEC 5
Radial play – 0.005 mm to 0.013 mm (0.0002 inch to 0.0005 inch)

Prior to testing, the bearings were inspected and passed per the following criteria:

1. Surface Appearance:
   - Lands, faces and mounting surfaces of bearing assemblies shall have a smooth finished appearance.
   - The surfaces shall be free of visible tool marks, chatter and waviness, pits, scratches with raised metal, or other surface imperfections.
   - Metal bearing components shall have a smooth finished appearance and shall be free of burrs, dents and folded material.
   - Non-metallic bearing components, including retainers, cages, and separators, shall be free of delaminations and burrs.
2. Cracks and fractures:
   - All bearing assemblies shall be free of cracks and fractures.
   - All bearing assemblies shall be free of scratches on critical surfaces.
   - All critical surfaces of bearing assemblies shall be free of scratches.
3. Contamination:
   - All exterior surfaces and interior areas of the bearing assemblies shall be free of foreign objects and debris, particles, fibers, grease, oil, fingerprints, etc.
4. Corrosion:
   - All exterior and interior surfaces of the bearing assemblies shall be free of corrosion, rust, and stains.
5. Assembly:
   - The proper number of rolling elements shall be present.
   - Retainers, cages, and separators shall be of the proper type (inner land-/outer land-/ball-guided), made of the proper material, and shall be installed in the proper orientation.

Lubricant

The bearings are commercial off-the-shelf. Their standard lubricant is not suitable for use at the low temperatures possible for this mechanism. After considering the potential operating conditions, we decided to remove the lubricant in the bearings and replace it with Castrol Brayco 815Z Micronic Grade Oil – a clear water white perfluorinated polyether-based fluid. We also selected alternate lubricants, but did not test them because our first choice was demonstrated to operate as desired.

The bearing retainer rings and shields were removed to allow inpsection of the bearing and observation of the meniscus during lubrication. The MIL-PRF-6085 oil was removed from the bearing components using heptane and a low intensity indirect ultrasonic cleaning technique. Previous investigation confirmed that this would not cause brinelling. We did not observe Brinelling using visual inspection at 10x magnification. Figure 1 shows one of the bearings after cleaning and drying.

Figure 1. Clean and Dry Bearing

Following the drying step, oil was injected into the clean bearing using a syringe for which the mass of each oil drop was established. The amount of oil was kept to the barest minimum to avoid making the bearing balls “snowplow” through a thick layer of cold oil.

Oil amounts were initally determined by consulting “A Space Tribology Handbook [2]” which states that a ball bearing with a 10-mm bore diameter takes less than 1 µL of oil to achieve a "starved" lubrication condition, and greater than 10 µL of oil to achieve a "flooded" lubrication condition. Beginning with these values each bearing was lubricated in three steps using the following guidelines:

- Papa Bearing with 2 drops (~6 mg or ~3.2 µL), 4 drops (~12 mg or ~6.4 µL), and 6 drops (~18 mg or ~9.6 µL) of Brayco 815Z oil,
- Mama Bearing with 1 drop (~3 mg or ~1.6 µL), 2 drops (~6 mg or ~3.2 µL), and 3 drops (~9 mg or ~4.8 µL) of Brayco 815Z oil, and
- Baby Bearing with ~2/3 drop (~2 mg or ~1.1 µL), ~4/3 drops (~4 mg or ~2.2 µL), and 2 drops (~6 mg or ~3.2 µL) of Brayco 815Z oil.

During deployment, the bearings operate for just a few seconds, so oil starvation is not a concern.

Oil mass for each bearing was selected iteratively by adding a drop of oil, running in the bearing to distribute the oil, and visually inspecting under magnification for both the presence of an oil meniscus between the

bearing balls and both inner and outer ring raceway grooves, and a thin film of oil fully coating the inner and outer ring raceway grooves. When a thin film and a meniscus was observed, the iterations were stopped and the total mass of oil added was determined and recorded.

The bearings were weighed dry and then again afterwards in order to measure the oil mass. This oil mass for each bearing was as follows:

- Papa Bearing – 13.6 mg
- Mama Bearing – 9.5 mg
- Baby Bearing – 4.3 mg

Figure 2 shows a microscopic view of one of the bearings indicating that the oil formed a meniscus between the ball and the raceway grooves. The view is looking towards the outer ring raceway groove. The body of the retainer crosses the lower right portion of the image. The ball has the curved bright highlight and is towards the upper right of the image. The meniscus is the narrower curved highlight just above that. The curved outer ring raceway groove can be discerned by the circumferential grinding marks extending towards the upper right corner of the photograph. The outer ring face sweeps diagonally across the upper left portion of the photograph.

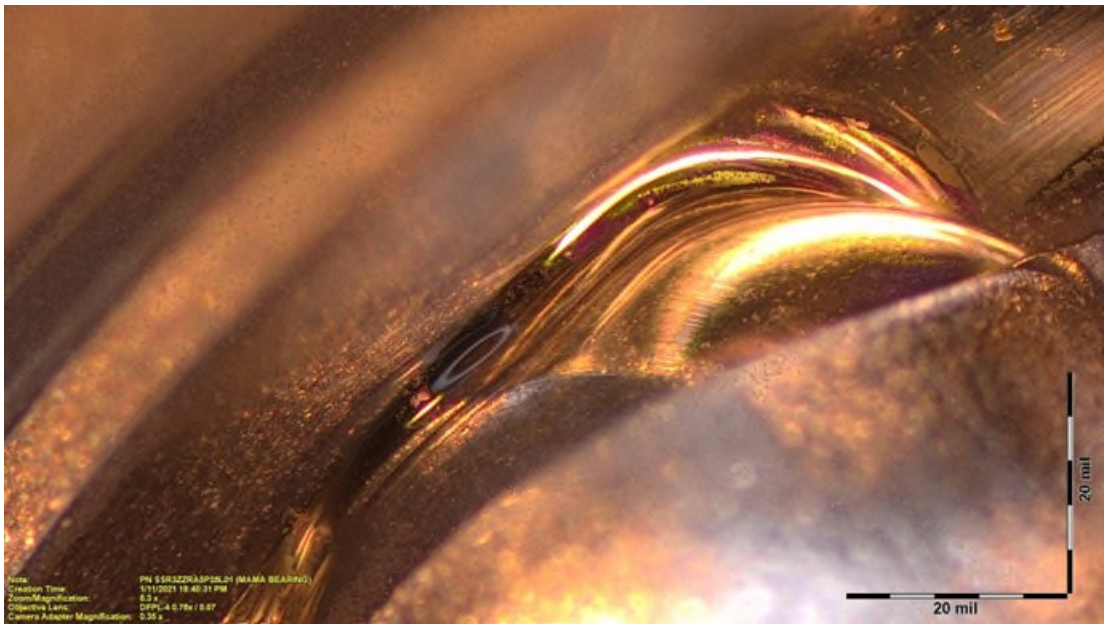

Figure 2. Microscopic View of Bearing Showing Oil Meniscus

Test Apparatus

We chose to use a commercially available VIBRAC BRG-3000 Bearing Inspector II tabletop bearing torque measurement apparatus that we already owned and was readily available. Rather than modifying this apparatus to operate inside a cooled thermal chamber, we elected to design a small insulated chamber that would encapsulate the bearing and provide insulated mechanical connections between the apparatus and the interior of the small chamber. This allowed us to keep the test apparatus at room temperature.

The torque tester has a motor that is controlled by the VIBRAC software to turn a shaft connected to the inner ring of the bearing while the outer ring was restrained by the torque transducer that measures the reaction torque at the outer ring as the inner ring i turned in a controlled manner using the software provided with the testing apparatus.

The experimental setup is shown in Figure 3. The insulated test chamber is the white cylinder with the access door labeled. The torque measurement apparatus consists of the base at the bottom containing the drive motor and the torque transducer near the top of Figure 3. The apparatus includes a structural tower supporting the torque transducer from the base. Just to the right of the torque transducer is a linear displacement sensor used in aligning the upper part of the apparatus to the lower part. On the upper right side of Figure 3 is the thermostatic controller for the liquid nitrogen flow. Below that, you see the plumbing for mixing and controlling the flow of gaseous and liquid nitrogen prior to passing through the wall of the insulated chamber to injection nozzles inside.

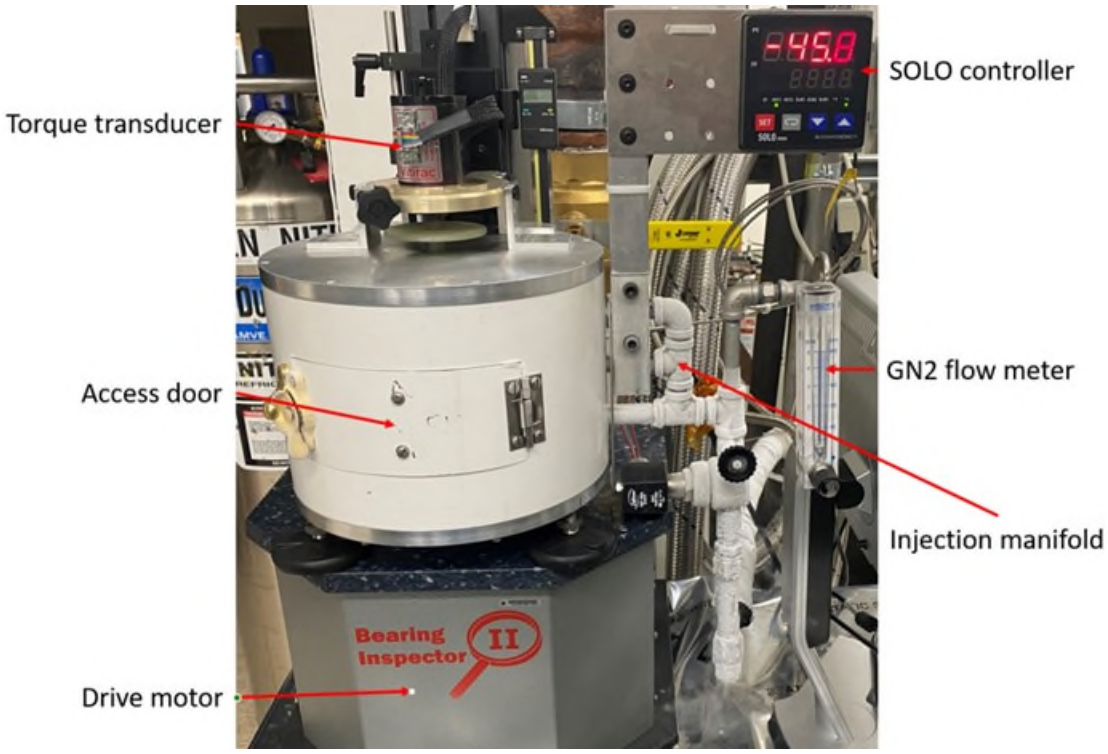

Figure 3. Test Apparatus

The cold chamber was constructed using Schedule 40 polyvinyl chloride (PVC) with 25-cm (10-inch) diameter outer wall and 20-cm (8-inch) diameter inner wall with rigid 80-kg/m^3 (5-lbm/ft^3) PVC foam insulation between the walls. The top and bottom of the inner tube were capped by 3-mm (0.125-inch) thick aluminum discs counterbored into the end of the tube. For the upper and lower caps, 13-mm (0.5-inch) plates of aluminum were used. The plates were separated by a layer of rigid PVC foam 25-mm (1-inch) thick. An access door was cut through the walls and attached using a spring-loaded hinge and a latch.

Figure 4 shows the thermal chamber partway during fabrication. The cold gas manifold is also shown, but without the nozzles to divert the flow laterally.

Figure 4. Cold Chamber During Fabrication

Figure 5 shows the apparatus assembled as it would be inside the thermal chamber. Resting on the right hand side of the baseplate of the testing unit are two of the three bearings along with insulating holders of G10 fiberglass (greenish) and Vespel polyimide (brown). Each bearing has its own customized mounts machined to match the dimensions of the bearing and attach it to the testing machine while providing thermal insulation to allow the testing machine to remain at room temperature. The third bearing is already installed in Figure 5.

Figure 5. Test Appartus Without Thermal Chamber

The large piece of copper is a 2.3-kg (5-lbm) weight that rests on the outer ring of the bearing to provide axial load across the bearing to approximate the loading condition it will experience in the mechanism. The

copper weight rests with its center of mass lower than the bearing to avoid any tendency to topple. The drive motor is inside the base and turns the shaft at the bottom.

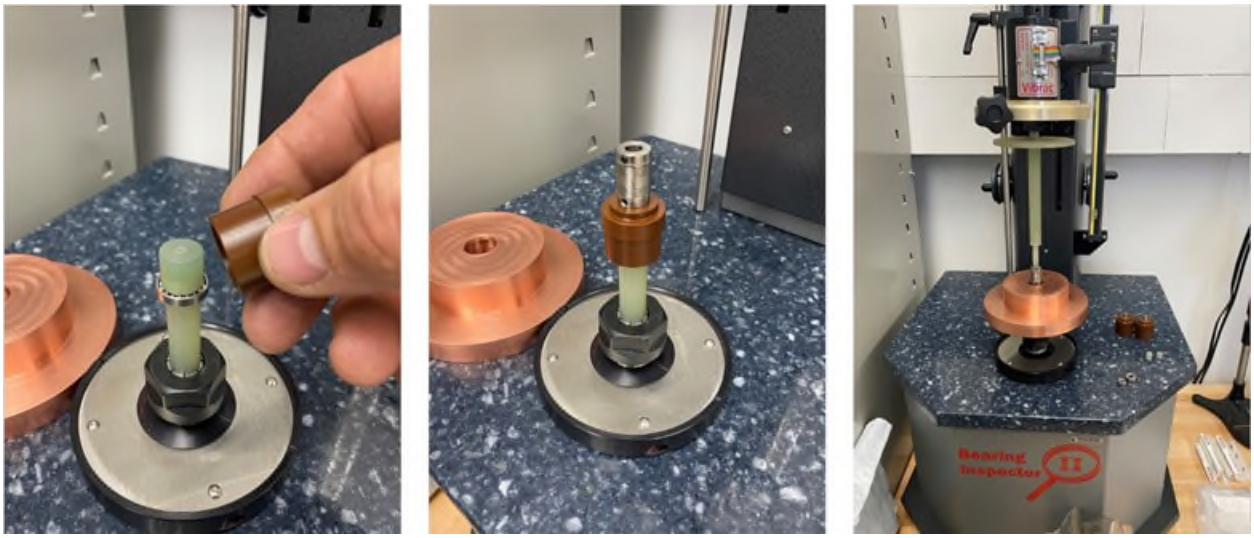

Figure 6. Bearing Support and Connection to Torque Tester

Figure 6 shows a sequence of photographs at successive stages of connection of the elements attaching the bearings to the torque tester. The attachment elements were machined out of G10 (green) and Vespel (brown) to provide mechanical connections while maintaining good thermal isolation. A G10 rod extends from the drive motor collet to the inner bearing ring. The inner bearing ring is captured by a slip fit cap axially clamped by a threaded fastener. The outer bearing ring is then captured using the Vespel cap. The stepped Vespel flange is arranged to support the 2.3-kg copper weight. A bellows-type flexible coupling then attaches the Vespel cap to the G10 rod that extends out the top of the chamber and to the torque transducer. The large G10 disk machined into the shaft protects the torque transducer from the cold nitrogen gas that flows upward around the shaft and out the hole in the top of the chamber. The disk diverts the flow out away from the torque transducer.

Test Operation

During testing, the chamber was cooled using cold nitrogen gas injected tangentially through three nozzles inside the chamber. The cold gas was created by mixing room temperature nitrogen gas with liquid nitrogen. The flow of the room temperature gas was adjusted manually to a desired constant flow rate using a rotameter. The flow of the liquid nitrogen was controlled in an on/off fashion using a solenoid ball valve controlled thermostatically by a SOLO 9696 controller that was also readily available in our lab space. During testing, we found that the flow of gas caused mechanical noise that was picked up by the sensitive torque transducer. Therefore, we temporarily turned off the flow of gas for a few seconds while taking a measurement. This worked quite well and allowed us to acquire reliable measurements of the starting torque.

The test apparatus was programmed to apply an angular acceleration of 0.050°/s^2 up to an angular speed of 0.39°/s for 3° rotation tests and 0.50°/s for 5° rotation tests. This was adequate to measure the starting torque of the bearing as well as to overcome the wind-up in the torque transducer

For each bearing, three measurements were taken in the clockwise direction and three were taken in the counterclockwise direction.

Observations

During early testing, we observed some angular oscillation in the time history as the bearing started to turn. This led us to investigate in more detail how the torque transducer works internally rather than just treating it as a “black box.” Based on a diagram in the manual [4], we learned that the torque transducer principle of operation uses two rods acting collectively as a torsional spring connecting two disks. When torque is applied, one disk rotates a small amount relative to the other disk and the rods bend slightly. This relative rotational deflection is proportional to the applied torque, and is measured optically. It required about 0.5 deg of rotation to wind up this torsional spring before the torque reached the starting torque being measured. The torque transducer was connected to the “fixed” outer ring with its deadweight disk. The small angular displacement of this “fixed” side led to a torsional pendulum action once the starting torque was overcome. For some operating conditions, the angular oscillations would feed back into the motor controller and the oscillations would continue. With a relatively large moment of inertia disk connected to a relatively soft torsional spring, the resonant frequency was just a few Hertz. We learned to test with angular displacements below 5 deg and many tests were programed for 3 deg, so the apparent instabilty never amplified enough to cause any issues. We also learned to keep the commanded angular acceleration very low. This ensured that there were no dynamic effects during the wind-up leading to startup in which the two rings of the bearing started to move relative to one another. The maximum measured torque from the first peak was taken as the measured starting torque even if subsequent peaks were higher. This test apparatus is often used to measure continuous running torque and does not normally have a weight connected with a large moment of inertia, so we did not anticipate this effect prior to our testing. While it was interesting to observe this small dynamic effect, this motion all occured after the measurement of the starting torque.

Figure 7 shows a sample time history of the measured torque during a test. In this case, the total angular displacement applied was 3 deg. The initial rise during the first half second is indicative of the wind-up torque of the torque transducer. Near the top of that first peak, the bearing begins to turn and the measured starting torque is about 0.92 mN·m (0.13 in·ozf). The drop after that is mostly due to release of the strain energy in the torque transducer. The rise back to about 0.64 mN·m (0.09 in·ozf) is more indicative of the running torque of the bearing. We were not making any attempt to measure the running torque, however, as our interest was focussed on the starting torque.

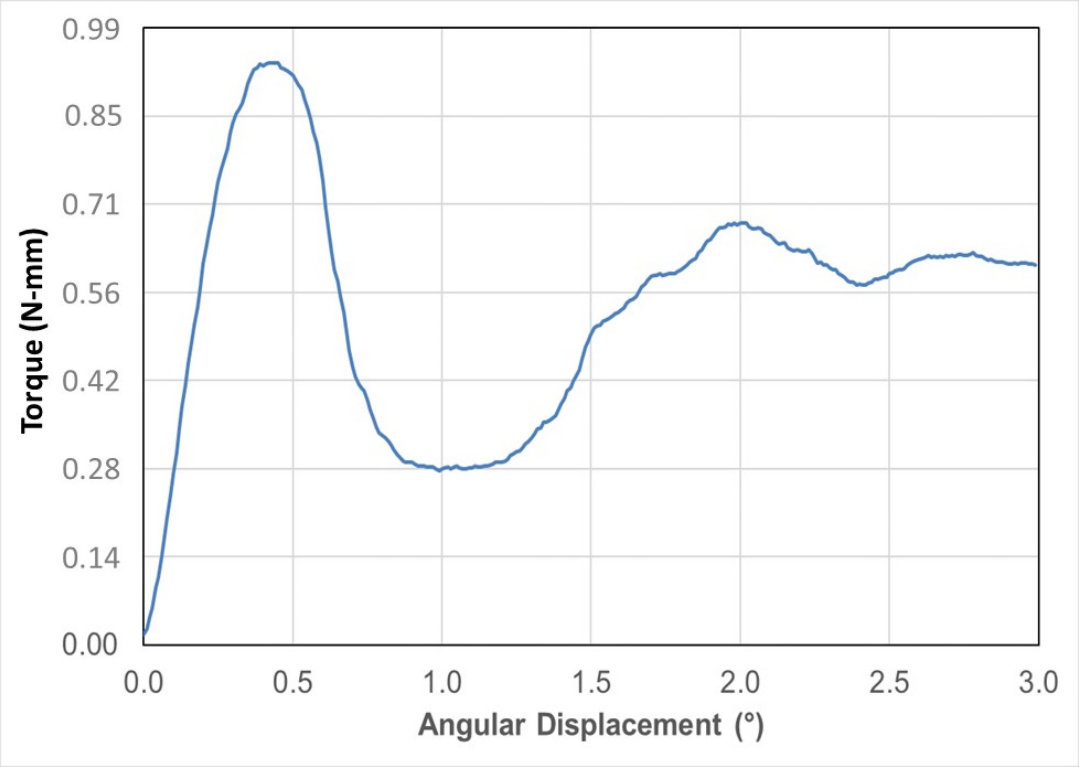

Figure 7. Sample Torque History

Test Results

The results of the testing confirmed that the torque needed to overcome the resistance of the cold lubricant was significantly smaller than the driving torque available from the mechanism. The coldest anticipated operating temperature for the mechanism is -70°C. The qualification testing of the antenna will be performed at a lower temperature of -85°C to demonstrate adequate margin. However, the resisting torque measurements were performed down to -90°C and -100°C. Although it was apparent that the starting torque was increasing rapidly as temperature was lowered, even at -100°C there was still adequate torque margin to overcome the breakaway torque of the bearings.

Figure 8, Figure 9, and Figure 10 show the starting torque for the three bearings. Each point is the average of the six measurements, three clockwise and three counterclockwise. There was no systematic dependence on direction of rotation, and the variability within each set of six measurements was less than ~10% of the average value plotted. As the temperature is decreased, there is a small trend of increasing torque, with a relatively large increase for temperatures below -70°C. This is not surprising since the pour point for the oil is -72°C. These tests also confirmed that the amout of oil applied to the bearings had been selected appropriately for this application. No further developmental testing is needed.

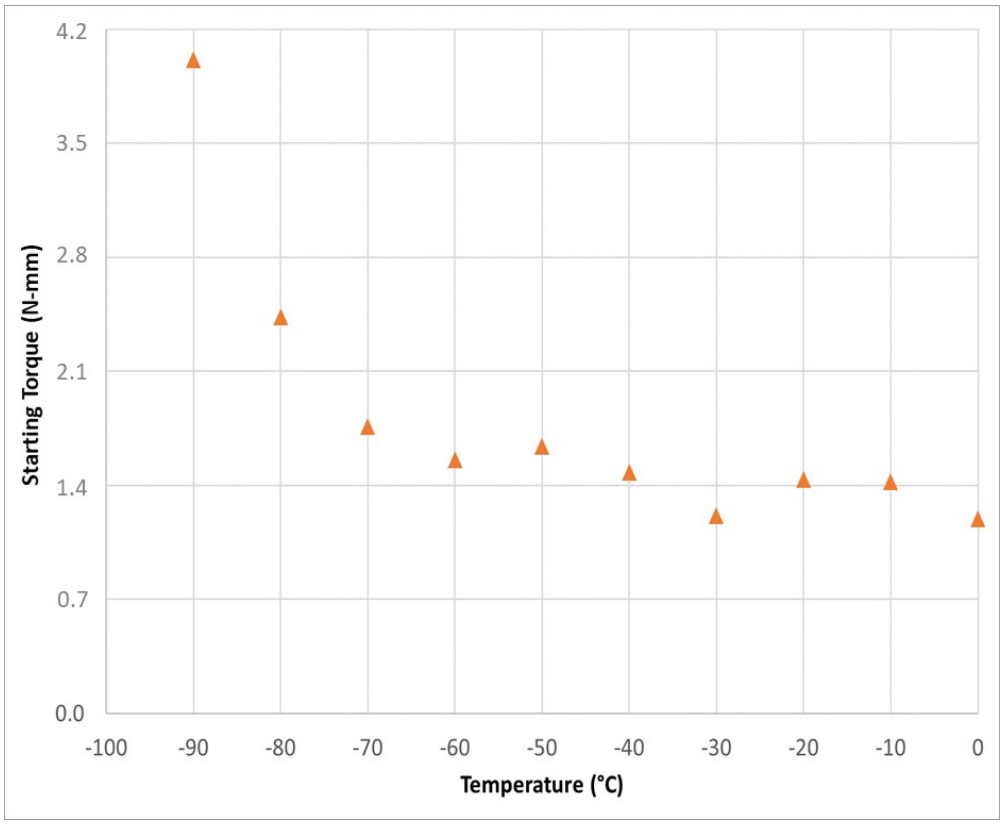

Figure 8. Starting Torque for 19.05 mm OD x 12.70 mm ID x 3.94 mm W (Papa) Bearing

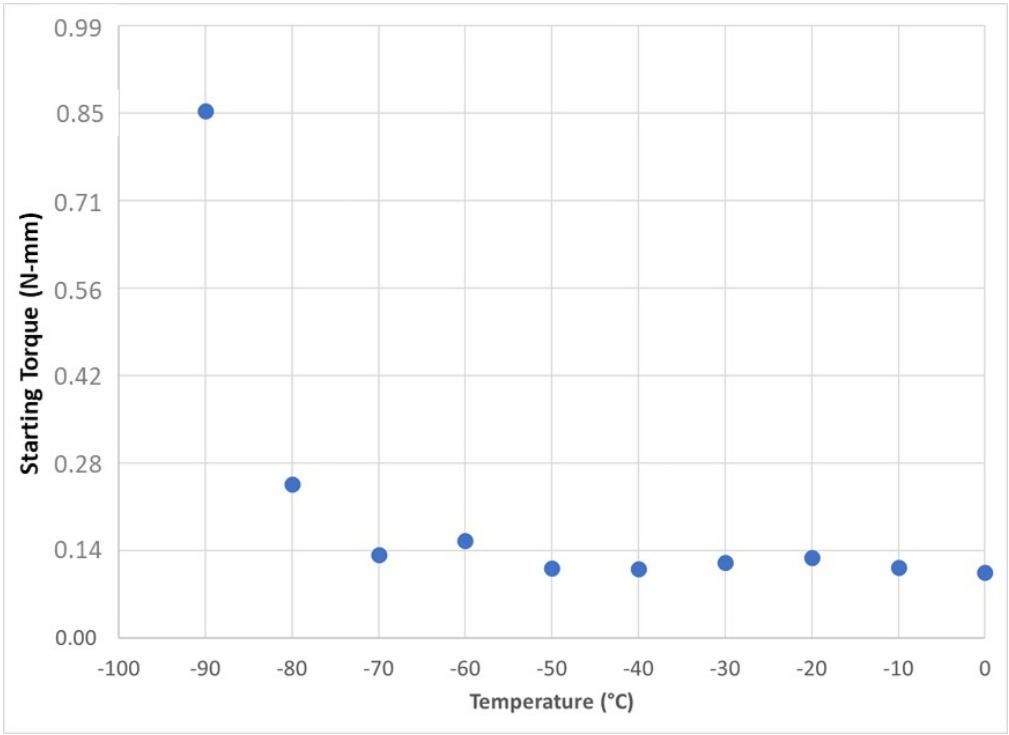

Figure 9. Starting Torque for 12.70 mm OD x 4.70 mm ID x 4.95 mm W (Mama) Bearing

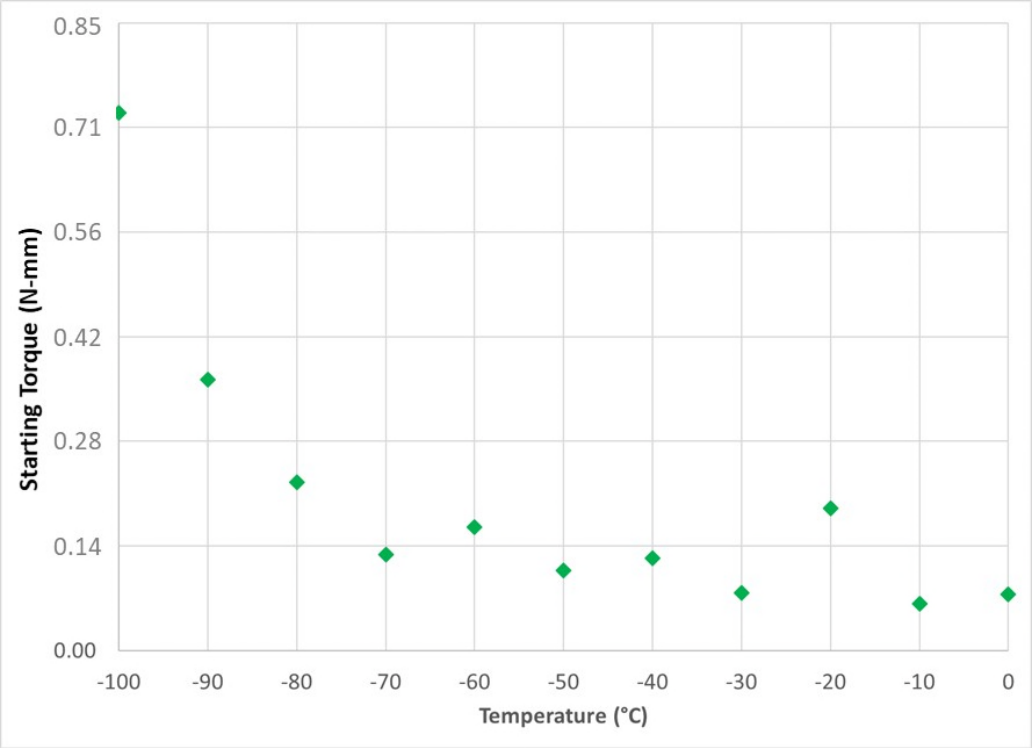

Figure 10. Starting Torque for 9.53 mm OD x 3.05 mm ID x 3.96 mm W (Baby) Bearing

Summary

Starting torque was measured at temperatures from 0°C to -90°C for two bearings and 0°C to -100°C for a third bearing. The oil selected is rated for operation down to -72°C and these measurements confirmed that the starting torque was quite consistent down to this temperature. Since the expected operating temperature of these bearings during deployment of the radar antennas of the REASON instrument could be below the rated temperature, we measured starting torque down to lower temperatures. These measurements retired a risk that the oil might increase in viscosity and cause more bearing drag than the mechanism could overcome at low temperatures. This gives us confidence that the mechanisms will be able to perform as needed during qualification testing as well as in space during the Europa Clipper mission.

Acknowledgement

The research was carried out at the Jet Propulsion Laboratory, California Institute of Technology, under a contract with the National Aeronautics and Space Administration (80NM0018D0004).

References

1. Castrol Brayco® 815Z Data Sheet. Retrieved March 9, 2022. https://msdspds.castrol.com/bpglis/FusionPDS.nsf/Files/C6FBF7AD844E7A6480257796002F8319/$File/Brayco%20815Z.pdf
2. Roberts, E. W., “A Space Tribology Handbook,” 7th European Space Mechanisms and Tribology Symposium, Proceedings of the conference held 1-3 October, 1997 at ESTEC, Noordwijk, the Netherlands. Edited by B. H. Kaldeich-Schürmann. ESA SP-410. Paris: European Space Agency, 1997., p.239, October 1997.
3. Bearing Inspector II Specification. Retrieved March 9, 2022. https://www.vibrac.com/bearing-torque-analysis-systems
4. Vibrac Torque Transducer Mini Series Specification. Retrieved March 9, 2022. https://www.vibrac.com/torque-transducer-mini-series